Aust. J. Phys., 1990, **43**, 499–517

Applications of Low-energy Electron Diffraction to Ordering at Crystal and Quasicrystal Surfaces*

E. G. McRae[A] *and R. A. Malic*

AT&T Bell Laboratories,
Murray Hill, NJ 07974, U.S.A.
[A] Retired.

Abstract

The value of the low-energy electron diffraction (LEED) technique for the evaluation of surface ordering depends on the ability to measure the intensity profiles of diffraction beams with respect to the associated surface component of the electron momentum transfer. Beam profiles, if measured with sufficient accuracy, may be interpreted to characterise the extent of surface order (e.g. distribution of step spacings) and to differentiate between different modes of disordering (e.g. surface melting versus roughening). The ability to measure LEED intensity profiles has been enhanced by use of low-current well-defined primary electron beams in conjunction with position-sensitive detection (PSD) of the diffracted electrons. The following are examples of applications of LEED–PSD. *Compositional Ordering at Ordering Alloy Cu_3Au (100) and (110) Surfaces:* The ordering of the (100) surface is believed to conform to a conventional picture in which the already-ordered bulk acts as a template, but the profiles measured in the course of ordering of the (110) surface are of the shapes expected if the ordering occurred first at the surface. *Disordering of Ge(111) Surface 150 K below the Bulk Melting Temperature:* The intensities and profiles are inconsistent with surface melting or roughening, but a model based on molecular dynamics simulations is not ruled out. *Order and Disordering at Decagonal Quasicrystal $Al_{65}Cu_{15}Co_{20}$ Surfaces:* At room temperature the quasicrystalline order is well developed at both the 'ten-fold' surface (perpendicular to the ten-fold surface (perpendicular to the ten-fold periodic axis) and a 'two-fold' one (parallel to the ten-fold axis) as evidenced by narrow beam profiles. The ten-fold surface undergoes a disordering transition at 700 K, but the temperature dependence of the profiles is unlike that expected for the roughening transition anticipated theoretically.

1. Introduction

The ability to monitor two-dimensional order has an important role in the characterisation of solid surfaces (Lagally *et al.* 1988). The observation of discrete beams in surface-sensitive diffraction experiments such as low-energy electron diffraction (LEED) is an indication of two-dimensional ordering, and the degree of order may be inferred from the intensity profiles of diffraction beams with respect to the surface-parallel momentum transfer (Van Hove *et al.* 1986).

A familiar example of this is the assessment of a surface by inspection of its LEED pattern as conventionally displayed on a fluorescent screen. If the surface has crystalline order, the pattern will be made up of discrete spots

* Paper presented at the Workshop on Interfaces in Molecular, Electron and Surface Physics, held at Fremantle, Australia, 4–7 February 1990.

0004-9506/90/040499$03.00

whose spacing is related inversely to the dimensions of the unit mesh. As described in this paper, quasicrystalline order also results in discrete spots in LEED patterns. In either case, a well-ordered surface will have a 'sharp' pattern—one made up of beams with narrow profiles—while a poorly-ordered one will have a 'fuzzy' or 'streaky' pattern due to beams with broader profiles.

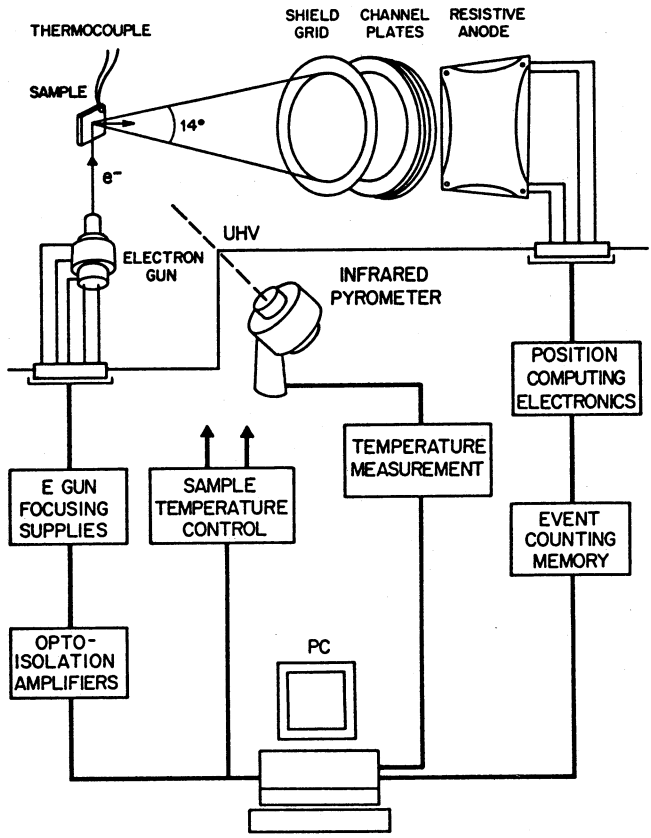

Fig. 1. Schematic of the LEED–PSD experimental arrangement. The PSD head (top right) is located in the ultra-high vacuum (UHV) envelope. The output of the position-computing electronics is routed to a personal computer (PC) which also controls the electron gun (e gun) and sample heater supplies.

In the last few years, the means have become available to refine and quantify this kind of assessment of surface order, while retaining the advantages of the display mode of observation. The essential requirements are a position-sensitive detector (PSD) and computing equipment capable of handling the large amount of data represented by a LEED–PSD image (McRae *et al.* 1985; Malic 1988). The LEED–PSD method of measuring beam intensities and beam profiles is being developed as an alternative to methods currently in use which employ a moveable Faraday collector (Lagally and Martin 1983) or beam deflection past a fixed aperture (Scheithauer *et al.* 1986). In this paper we describe the LEED–PSD method, and we summarise applications to the determination of ordering at crystal and quasicrystal surfaces.

2. Experimental Procedures

The important advantages of PSD over the conventional fluorescent-screen detection derive from its thousand-fold greater efficiency. Since practically every diffracted electron arriving at the detector is counted, it is feasible to observe LEED with very low-current incident beams (typically 10^{-12} A) which are relatively easy to collimate and focus. The use of a well-defined incident beam permits observations of beam profiles with improved resolution with respect to surface-parallel momentum transfer and consequent refinements in the description of surface order.

A LEED–PSD set-up is shown in Fig. 1. The PSD used in our experiments consists of a grounded fine-mesh grid, a pair of 75 mm-diameter channel electron multiplier arrays (channel plates) and a resistive anode, together with electronics that compute the position of arrival of electrons at the first CEMA by comparing the charges at the anode corners (Surface Science Laboratories, Palo Alto, CA). An analogue display of the output is provided. The digital output is buffered by a specially-built event-counting memory (Erbtec Engineering, Boulder, CO) and eventually down-loaded to a Sun workstation for analysis. The maximum data rate of the detector is 10^5 s^{-1} with 256×256 channel positional resolution. The electron gun is fitted with a sharply pointed filament (Ebtec, Agwam, MA) providing a relatively small electron source. The overall instrumental resolution as measured by the coherence zone diameter is at least 500 Å. This lower limit was determined by measuring the widths of profiles of beams from a well-ordered Si(111) surface.

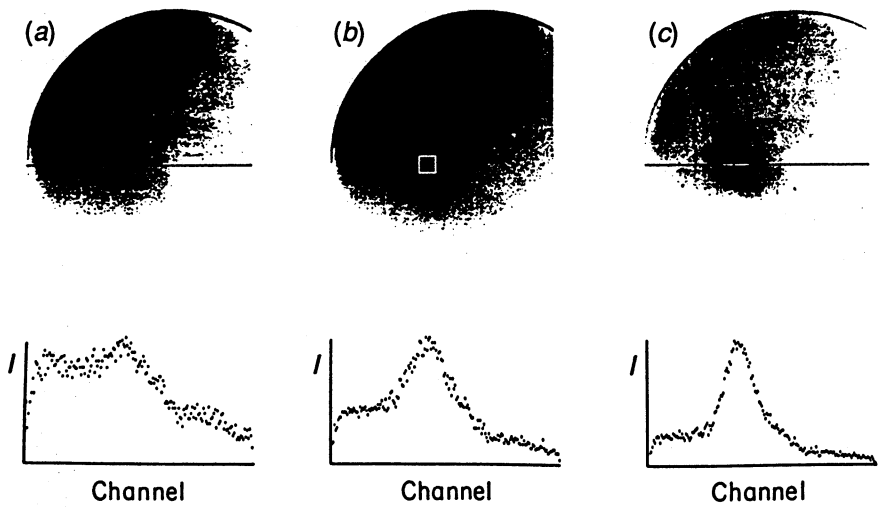

Fig. 2. Displays of the intensity distribution within a superlattice diffraction spot from a $Cu_3Au(110)$ surface in successive stages of ordering: (*a*) early, (*b*) intermediate and (*c*) late stages. Grey-scale (top) and profiles (bottom) are shown, with the profiles along the lines indicated in (*a*) and (*c*). The square in (*b*) is one of the integration ranges used in the analysis described in Section 2.

Examples of LEED–PSD records of a beam at three stages of progressive surface ordering are shown left to right in Fig. 2. These records are displayed and analysed using an image analysis program (Kropfl 1989) running on

the Sun workstation. The intensity background apparent especially in the normalised profiles at the lower part of the figure is due to the quasi-elastically scattered electrons passed by the retarding field in front of the first CEMA. The presence of this background—unavoidable in any display-type LEED measurement—is the most serious disadvantage of the LEED–PSD method. Special data-reduction procedures including background subtraction are being used to extract information about surface ordering.

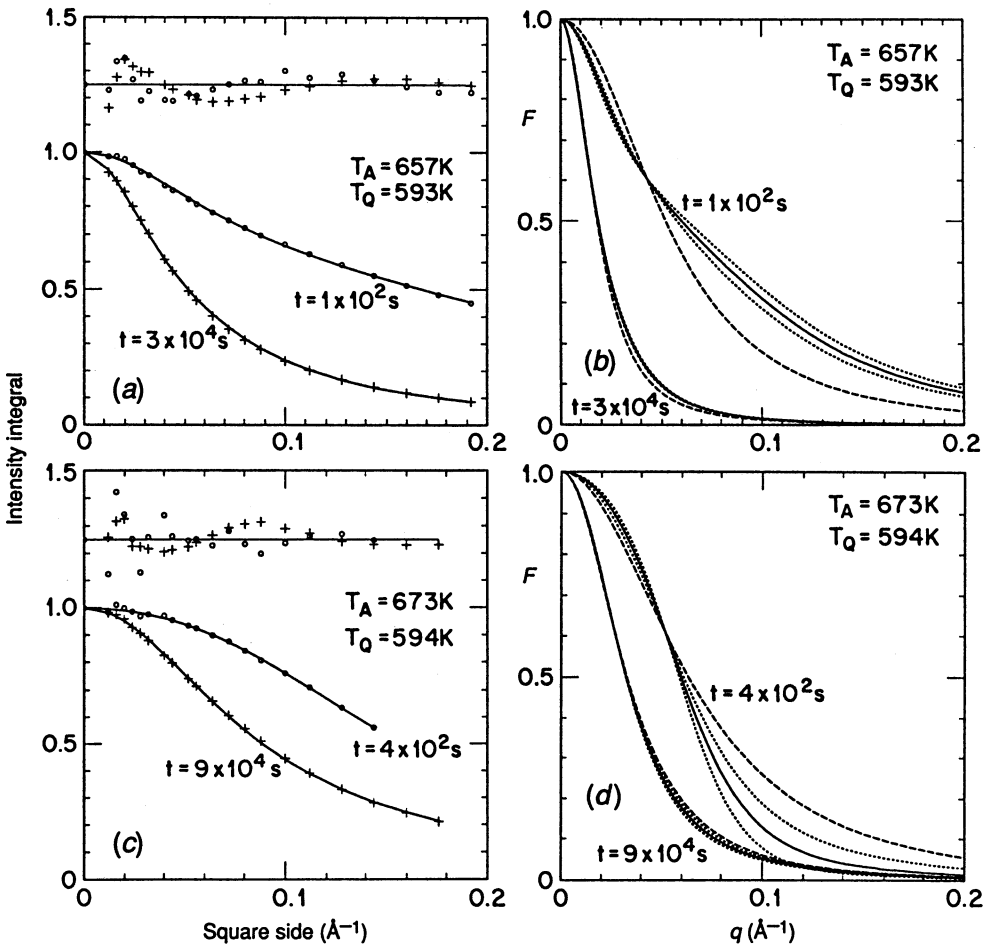

Fig. 3. Intensity integrals (left) and intensity profiles derived from analysis of the intensity integrals (right) for a superlattice beam from a $Cu_3Au(110)$ surface in early (small time t) and late (large t) stages of ordering. Here $F(q)$ denotes the profile function where q is the surface-parallel momentum transfer, T_Q denotes the temperature at which ordering was observed as a function of t, and T_A denotes the temperature of the ordering anneal prior to quenching to T_Q. In (*a*) and (*c*), difference plates (×10, shifted up 1·25) are shown. Curves indicate best fits to the data using a trial profile function. In (*b*) and (*d*), solid curves indicate profiles yielding best fits to data, dotted curves indicate envelopes of lines lying within 95% confidence limits for estimation of parameter values, and dashed curves indicate a standard profile (Lorentzian to the power 3/2).

One data-reduction procedure evaluates three beam parameters in a way that makes optimal use of the intensity data. The procedure is limited to approximately round spots. The parameters are the height to the peak (peak intensity) I_P, the width of the peak q_1, and the profile shape parameter q_2 (McRae and Malic 1990). The shape parameter is a measure of the pointiness of the profile relative to a standard profile shape such as a Lorentzian to the power 3/2 (L3/2); a negative value of q_2 corresponds to a profile that is pointy-topped, and a positive value to one that is flat-topped relative to L3/2. The procedure consists of comparing intensity integrals over successively larger squares like the one illustrated in Fig. 2*b*, with the corresponding integrals for trial profile functions. Fig. 3 shows examples of intensity integrals and of beam intensity profiles determined in this way.

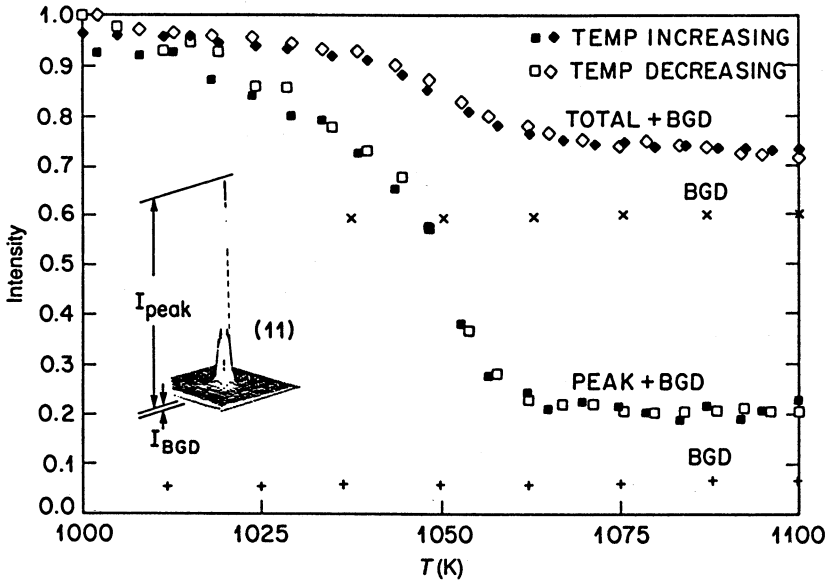

Fig. 4. Determination of total and peak spot intensities over a range of sample temperatures spanning that of a surface disordering transition. The total (integrated) intensity within the window indicated in the inset, the peak intensity and the respective background (BGD) intensities are represented, the former for both increasing and decreasing temperature. The data shown are for Ge(111) surface, (11) spot. The transition temperature is 1060 K.

A second procedure evaluates the total intensity I_T inside a square centred on the beam as in Fig. 2*b*. This is useful in monitoring the appearance and disappearance of weak beams for varying conditions in the vicinity of a surface phase transition. Instead of using the image analysis program it is more efficient in this case to use the windowing capability of the position-calculating electronics to define the areas of interest in the analogue display. A ratemeter is used to measure the intensity in a window centred on the beam, and the intensity in a similar nearby window is subtracted to evaluate I_T. Fig. 4 shows an example of the variations of total and peak intensities associated with a disordering transition at Ge(111) surface (see Section 4).

3. Applications to Cu_3Au Crystal

(a) Introduction

The nature of the surface phase transitions associated with a first-order transition of a bulk crystal has been the subject of theoretical speculation (Lipowsky 1982, 1984, 1986; Lipowsky *et al.* 1983; Binder 1983; Lipowsky and Gompper 1984; Sanchez and Moran-Lopez 1985*a*, 1985*b*; Majia-Lira *et al.* 1985; Cahn *et al.* 1987; Kroll and Gompper 1987; Moran-Lopez *et al.* 1985; Dietrich 1988; Gompper and Kroll 1989). The ordering alloy Cu_3Au, which undergoes a first-order compositional order–disorder transition at temperature T_0 near 663 K (Warren 1969), provides an experimentally convenient means of testing theoretical ideas about the relationship between bulk and surface ordering.

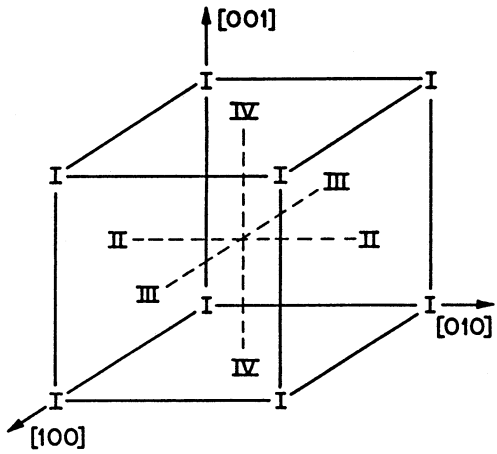

Fig. 5. Four equivalent superlattices I–IV of the Cu_3Au crystal in its compositionally ordered state. The fcc unit cube is shown, with positions of the Au atoms in the respective superlattices indicated.

(b) Bulk Order–Disorder Transition

In its ordered state, the Cu_3Au crystal is of the $L1_2$ superlattice type, in which the Au atoms occupy one of four equivalent superlattices of the fcc lattice (Fig. 5) (Warren 1969; Fontaine 1979). The transition at T_0 is to a disordered state in which the Au and Cu atoms are randomly located on fcc sites. The disordering transition as observed with X-ray diffraction consists of the abrupt drop of superlattice beam intensities at T_0. Its abrupt character corresponds to a congruent point in the phase diagram (Hansen 1958), at Au atom fraction $\frac{1}{4}$. For off-stoichiometric crystals with compositions close to Cu_3Au, the transition is smeared out by the temperature difference between the boundaries of the two-phase coexistence region (Rase and Mikkola 1975).

The process of ordering at temperatures just below T_0 has been studied (Sakai and Mikkola 1971; Nagler *et al.* 1988; Ludwig *et al.* 1988). In these

experiments the time required to restore a substantially ordered condition after a disordering anneal is of the order of 10^6 s. In the later stages of ordering, the partially ordered crystal is made up of well-ordered domains in each of which the Au atoms occupy predominantly one or other of the four sublattices. The domain dimensions increase with ordering time t in proportion to t^a, where a is a constant having a value close to 0·5 in accordance with theoretical expectation (Allen and Cahn 1979). The walls separating the domains are mainly of the type known as type I; the walls are parallel to the {100} unit-cube sides, and correspond to a relative shear displacement equal to half a cube-side diagonal (Wilson 1943; Cowley 1950; Yamaguchi *et al.* 1961). Type I domain walls (just 'walls' from here on) are of low energy because their formation does not involve any change of nearest-neighbour atomic configuration. The ordering of bulk Cu_3Au may be pictured approximately as annealing-out of walls. Walls are present even at equilibrium below T_0 in off-stoichiometric alloys with compositions close to Cu_3Au, e.g. Au-rich alloys (Sato and Toth 1962).

(c) (100) Surface Order–Disorder Transition

$Cu_3Au(100)$ has been the subject of experimental study (Sundaram *et al.* 1974, 1975; Potter and Blakely 1975; Buck *et al.* 1983; McRae and Malic 1984; Jamison *et al.* 1985; Alvarado *et al.* 1987; Dosch *et al.* 1988) and discussion (Lipowsky 1982, 1984, 1986; Sanchez and Moran-Lopez 1985*a*, 1985*b*; Dietrich 1988). The LEED pattern at temperatures below T_0 is that expected for the ideal termination of the ordered bulk crystal (Potter and Blakely 1975).

The compositions of the outermost two atom layers have been determined by low energy ion scattering (LEIS) (Buck *et al.* 1983). The Au atom fractions in (100) atom layers of the ordered bulk crystal are alternatively $\frac{1}{2}$ and 0. The LEIS results are consistent with a surface geometrical structure like that of an ideally-terminated fcc crystal. The Au atom fractions in the first and second layers were found to be 0·52 and 0·00 respectively. A sequence of nearly ideal layer compositions for the ordered bulk crystal extends to the surface, terminating in a Au-rich layer. Remarkably, the nearly ideal compositions were found to persist, not only below T_0 but to at least 50 K above T_0 as well. At higher temperatures the layer atom fractions only slowly approach the value $\frac{1}{4}$ for an ideally terminated disordered crystal. Compositional ordering with respect to the surface-normal direction is evidently preserved at temperatures well above T_0.

The surface transition has been characterised by LEED using position-sensitive detection (LEED–PSD) (McRae and Malic 1984). In contrast to the abrupt change at T_0 of the X-ray superlattice beam intensity from the bulk crystal, the corresponding LEED intensity I_P decreases smoothly with increasing temperature t in accordance with

$$M \equiv \sqrt{I_P} \propto (1 - T/T_1)^{\beta}, \tag{1}$$

where T_1 is an apparent critical temperature equal within error to T_0, and β is a constant. A fit to the experimental points (Fig. 6) is obtained with $\beta = 0{\cdot}23 \pm 0{\cdot}02$. Corresponding to this intensity variation, the component of

the LEED beam profile associated with fluctuations of compositional ordering narrows as T approaches T_1. The same temperature dependence of intensity and of profile shape are generally observed with temperature increasing and decreasing.

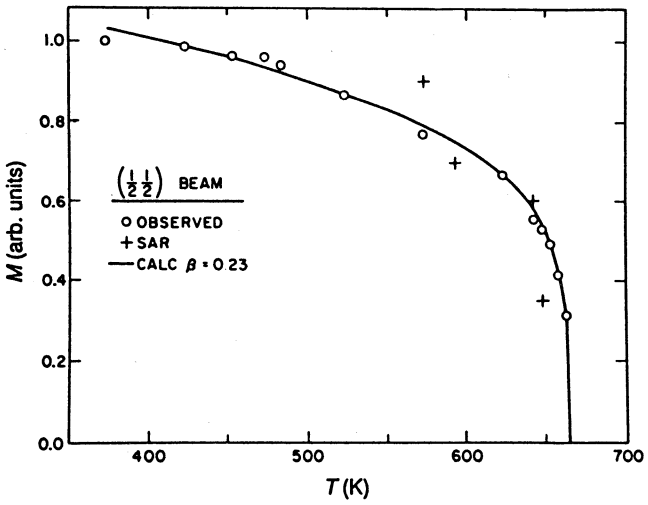

Fig. 6. Square root M of the intensity I_P of a superlattice spot in LEED from $Cu_3Au(100)$ as a function of sample temperature T. Data points from LEED–PSD (circles) are shown in comparison with earlier LEED results (SAR, Sundaram *et al.* 1975, crosses). The curve is calculated according to equation (1).

Experimental results such as described above, e.g. the value of β, generally depend to some extent on the crystal history. In preparing the surfaces used in the cited experiments (McRae and Malic 1984) it was found that the apparent value of β decreased upon prolonged annealing of the crystal. Thus, any experimental value should be accepted only as an upper limit of the true value for an initially ordered crystal. Annealing up to 100 h at temperatures just below T_0 may be necessary to achieve a stable condition, depending in a generally unknown way on the crystal history.

(d) (110) Surface Order–Disorder Transition

$Cu_3Au(110)$ has been the subject of experimental study (McRae and Malic 1990; Potter and Blakely 1975; Alvarado *et al.* 1987; McRae *et al.* 1990*a*; Krummacher *et al.* 1989). The results reviewed here refer to a surface that below T_0 has the LEED pattern expected for the ideal termination of the ordered bulk crystal (Potter and Blakely 1975). Other LEED patterns that have been observed, the 4×1 (McRae *et al.* 1990*a*; Krummacher *et al.* 1989) and incommensurate hexagonal patterns (McRae *et al.* 1990*a*) are not directly associated with the bulk compositional ordering.

The compositions of the outermost two atom layers have been determined by LEIS (McRae *et al.* 1990*a*). The Au atom fractions in (110) atom layers of the ordered bulk crystals are alternately $\frac{1}{2}$ and 0. The LEIS results are consistent with the surface geometrical structure like that of the ideally terminated fcc

crystal. The Au atom fraction in the first (second) atom layer was found to vary from 0·40 (0·20) at room temperature to 0·35 (0·35) at temperatures within 50 K to T_0. The possibility that the departures from ideal Au-rich termination might be due to the presence of domains with the ideal Cu-rich termination, separated by steps with height equal to one layer spacing, was ruled out by LEED observations showing the steps to be predominantly of height equal to two layer spacings. These results correspond to a net segregation of Au to the outermost two atom layers.

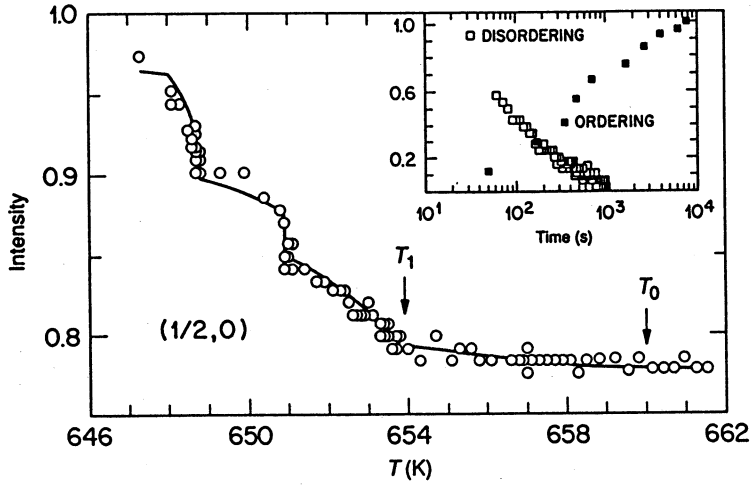

Fig. 7. Total intensity of a superlattice spot in LEED from $Cu_3Au(110)$ surface as a function of sample temperature T, where T_1 and T_0 denote the surface and bulk transition temperatures respectively. The measurements were made with T increasing, with pauses at 649, 651 and 654 K. The inset shows the time dependence of intensity at 649 K for T increasing (disordering) and T decreasing (ordering).

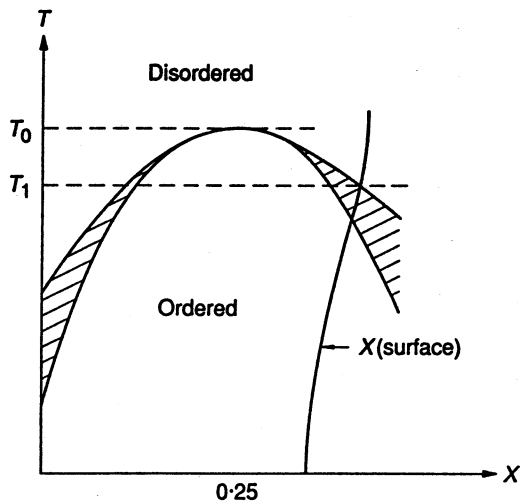

Fig. 8. Schematic phase diagram explaining the properties of the $Cu_3Au(110)$ surface phase transition. Here T and X denote the temperature and the Au atom fraction respectively, while T_0 and T_1 denote the bulk and surface disordering transition temperature respectively. The two-phase coexistence region is indicated by shading. The qualitative T dependence of the surface Au atom fraction is indicated by the curve X (surface). This curve crosses a coexistence region lying entirely below the congruent point at ($T = T_0$, $X = 0{\cdot}25$), thus accounting for a smooth decrease of intensity for T increasing up to $T_1 < T_0$.

The surface transition has been characterised by LEED–PSD (McRae and Malic 1990; McRae *et al.* 1990*a*). The superlattice beam intensity was found to decrease linearly with increasing crystal temperature, and die out at temperature T_1 6 K below T_0 (Fig. 7). The transition exhibits marked hysteresis due to a relatively low rate of ordering. On the basis of the asymmetry between rates of ordering and disordering, the transition was identified as first order. The slow variation of intensity near T_1 was explained by analogy with the off-stoichiometric bulk transition (Fig. 8). This analogy is plausible in view of the observed surface segregation of Au.

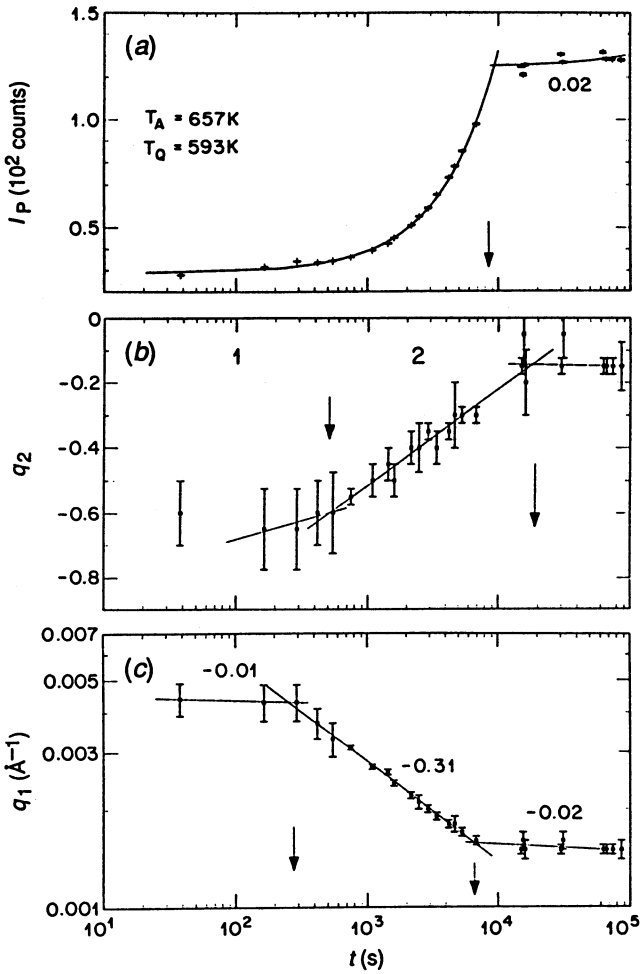

Fig. 9. LEED–PSD observations of ordering at the $Cu_3Au(110)$ surface. The evolution of the intensity and profile parameters with respect to ordering time t occurs in two distinct regimes 1, 2 terminated at times indicated by arrows. Here T_A denotes the temperature of the ordering anneal preceding the quench to the ordering temperature T_Q. The lines indicate (*a*) exponential or (*a*)–(*c*) linear fits to the data. Error bars correspond to the dimensions of a rectangle enclosing the 95% confidence contour in fitting the data. Numerals indicate the slopes of the linear fits.

Observations of ordering kinetics were reported, corresponding to two different initial conditions of disorder: (*a*) disordered surface on an ordered substrate, achieved by annealing at a temperature T_A between T_1 and T_0; (*b*) disordered surface on a disordered substrate, by annealing above T_0 (McRae and Malic 1990). The times required to restore the surface to a substantially ordered condition after annealing and then quenching to a temperature $T_Q < T_1$ were (*a*) 10^5 s and (*b*) 10^6 s. The latter figure is comparable with the bulk ordering time.

(e) Role of Type I Domain Walls in (100) and (110) Surface Transitions

The energetic equivalence of the three geometrically distinct type I domain walls need not apply near a surface; their energies may vary depending on their orientation to the surface. It has been suggested that the striking differences between the properties of the low-index surfaces of Cu_3Au derive from the effect of the surface in lifting the degeneracy of walls (McRae and Buck 1990). The (100) surface has a special place in this discussion because it is parallel to one of the walls. The assumption that the surface-parallel wall is relatively stable permits a rationalisation of the very different surface compositions and ordering kinetics at the (100) and (110) surfaces.

(f) Detailed Study of (110) Surface Ordering Kinetics

Plots of the superlattice spot parameters I_P, q_1 and q_2 against ordering time t indicate the existence of two distinct ordering regimes (recall from Section 2 that I_P, q_1 and q_2 refer to the peak intensity, the width and the profile shape). This is illustrated in Fig. 9 for a particular combination of values of annealing temperature T_A and ordering temperature T_Q. Let t_1 and t_2 denote the times at the end of the first (early) and second (late) regimes (indicated by arrows in Fig. 9). The beam profile shapes in the early regime are qualitatively different for the two initial conditions of ordering. For initial condition (*a*)—ordered substrate—which is represented in Fig. 9, the profiles are pointy-topped, while for initial condition (*b*)—disordered substrate—they are flat-topped. In the late regime the profile shapes approach L3/2 for both initial conditions. The durations t_n of the regimes ($n = 1, 2$) have an approximately exponential dependence on T_Q^{-1}: $t_n \approx A_n \exp(B_n/T_Q)$ where A_n and B_n are constants. This is indicated by the nearly linear plots of $\ln t_n$ in Fig. 10. The slopes of these plots correspond to apparent activation energies of ordering $B_n k_B$ (k_B is Boltzmann's constant) in the range of possible diffusion activation energy values for Cu_3Au (1·5–2·0 eV) except for the early regime for initial condition (*b*)—disordered substrate. In that exceptional case the value of activation energy for ordering is twice that for diffusion. These results have been interpreted as follows:

(*a*) The ordered substrate provides a template on which the surface orders by the net migration of surface atoms to sites energetically favourable to their type. Since the substrate is ordered, for $t > 0$ and $T_Q < T_1$ there is always an excess of atoms in 'right' sites over those in 'wrong' sites. Correspondingly there is long-range order and this results in a delta function component and consequent pointy-topped character of the beam profile.

(*b*) Since the substrate is disordered, long-range order is initially absent but the surface can develop short-range order as a result of concerted motions of pairs of surface atoms to form small ordered domains. The flat-topped character of the profiles is consistent with the absence of long-range order and also suggests that distribution of domain size is sharply peaked at a particular size. The value of the profile width parameter q_1, which varies little through the early regime, indicates a mean domain diameter about 20 Å.

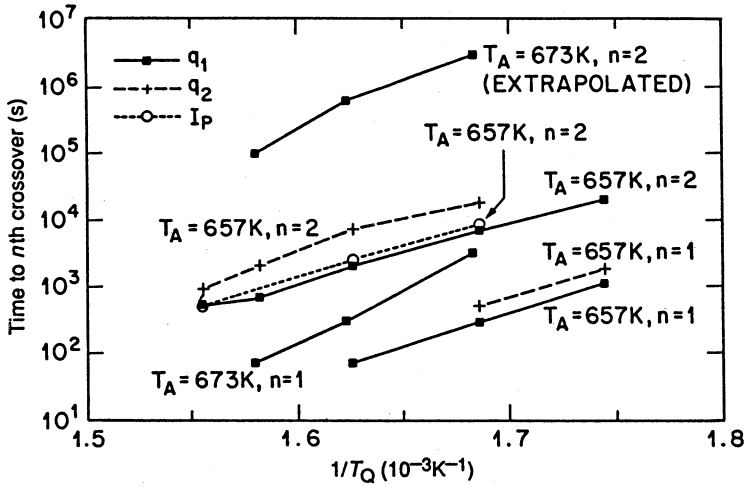

Fig. 10. Dependence on reciprocal sample temperature T_Q on the time t_n to the nth crossover (end of the nth regime, $n = 1, 2$) in the ordering of the $Cu_3Au(110)$ surface. The parameter plots used in evaluating t_n are identified at top left. Here T_A denotes the annealing temperature prior to the quench to T_Q.

4. Application to the (111) Surface of Ge Crystal

The existence of various surface reconstructions of the Ge(111) surface and of transitions between these ordered surface phases have been known for a long time, but LEED–PSD experiments have revealed a new transition in which the lateral crystalline order at the surface is extinguished at temperatures within 160 K of the bulk melting temperature (McRae and Malic 1988). Previously only indirect evidence of this disordering transition was available (Lever 1968; Lever and Went 1970; Frantsuzov and Makrushin 1973).

The intensity versus temperature plots, introduced in Section 2 (Fig. 4) to illustrate procedures, are evidence of a disordering transition near 1060 K. These plots are for a non-specular beam, i.e. beam for which the surface-parallel momentum transfer $S_{||}$ is nonzero. Fig. 11 shows a series of intensity-temperature plots for the specular beam ($S_{||} = 0$) and for non-specular beams corresponding to successively larger values of $S_{||}$. There is no evidence of a transition for $S_{||} = 0$, and the intensity drop near 1060 K is more pronounced for increasing $S_{||}$. Since in these as in most LEED experiments the surface-normal momentum transfer is much greater than the largest value of $S_{||}$ encountered, the absence

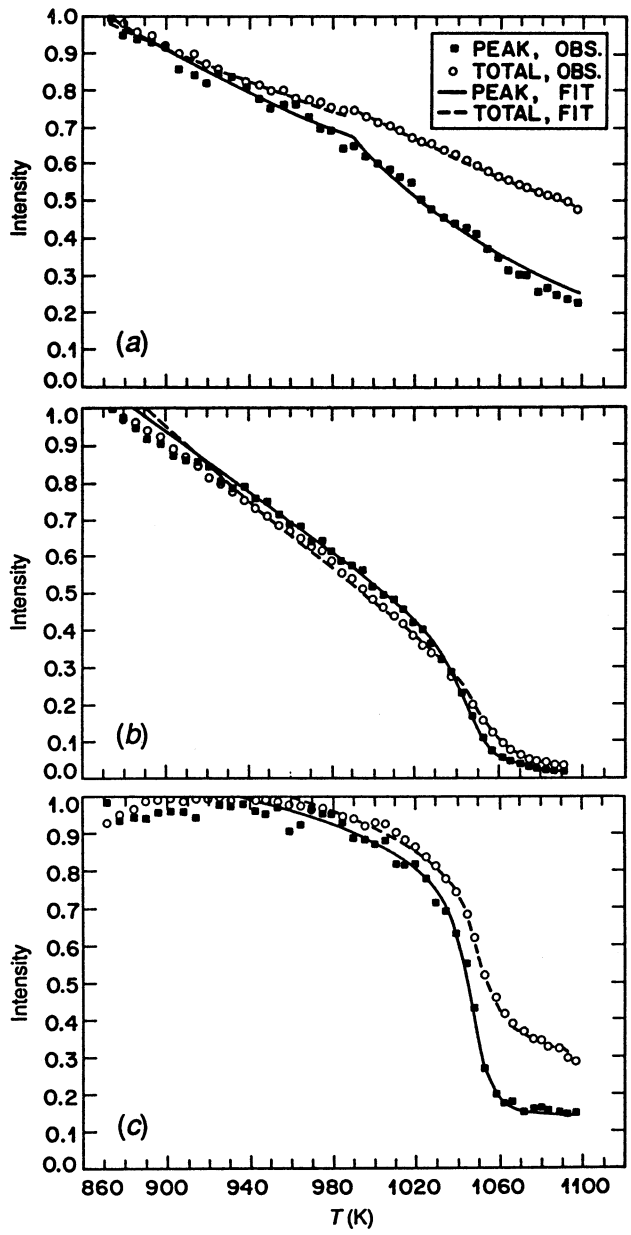

Fig. 11. Plots of peak and total spot intensity versus sample temperature for the Ge(111) surface. The spots represented correspond to the following values of surface-parallel momentum transfer: (*a*) $S_{||} = 0$, (*b*) $S_{||} = 1 \cdot 81$ Å^{-1} and (*c*) $S_{||} = 3 \cdot 14$ Å^{-1}. The curves in (*a*) are Debye–Waller lines corresponding to slightly different values of surface Debye temperature above and below 980 K. In (*b*) and (*c*) the curves are fits to the data by an expression incorporating a critical temperature $T_1 = 1060$ K (for details see McRae and Malic 1988).

of an intensity drop for $S_{||} = 0$ is evidence that the atomic displacements in the disordering are parallel rather than normal to the surface, i.e. the surface undergoes lateral disordering.

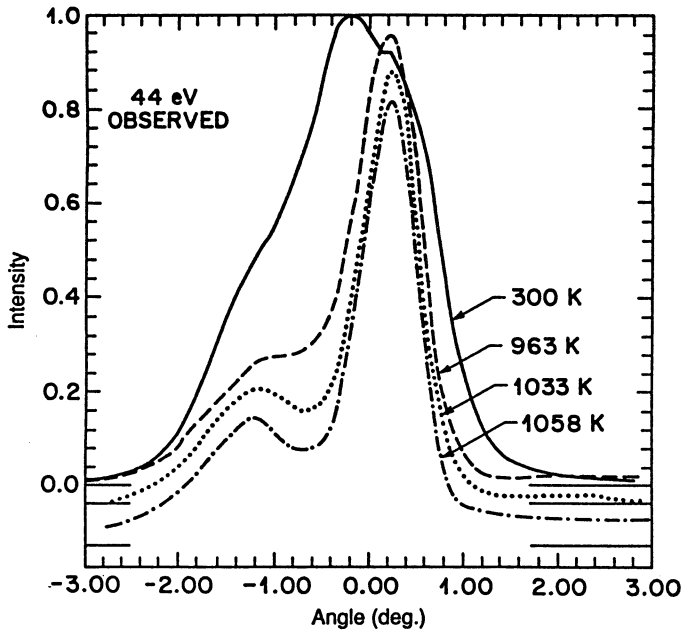

Fig. 12. Specular spot intensity profiles for Ge(111) surface at the indicated temperatures.

Two disordering mechanisms involving surface-normal displacements may be ruled out on the basis of the available evidence. A roughening mechanism would generally result in a broadening and change of shape of the beam profiles, but as illustrated in Fig. 12 the observed profiles are the same just above and just below the transition temperature. The shoulders on the profiles are due to steps with mean separation about 90 Å, and these shoulders would have moved had there been any significant change of the step separation as would occur in a roughening transition. A surface melting mechanism would result in a decrease of the specular beam intensity below the Debye–Waller curve indicated in Fig. 11. A third disordering mechanism suggested by molecular dynamics simulations for Ge(111) (McRae *et al.* 1988) is not ruled out by the experiments. In the disordered state of the surface the outermost double layer of Ge atoms forms laterally strained domains separated by filaments of amorphous or molten material. This model can account for the observation of increasing prominence of the intensity drop for increasing $S_{||}$ (McRae and Malic 1988).

5. Application to $Al_{65}Cu_{15}CO_{20}$ Quasicrystal

The structure and physics of quasicrystals are topics of intense and widespread current inquiry (Steinhardt and Ostlund 1987). These investigations have been limited to the bulk materials, but recently the ability to grow large and nearly-perfect samples of decagonal quasicrystals of $Al_{65}Cu_{15}Co_{20}$ (Kortan *et al.*

1989) has set the stage for studies of quasicrystalline surface ordering as well. Decagonal quasicrystals are of periodic layered structure where the individual layers are perpendicular to the periodic ten-fold axis. As these layers are thought to be realisations of a two-dimensional quasicrystalline tiling (Kortan *et al.* 1990), experimental information about the structure and stability of their surfaces is likely to have an important role in the evaluation of such two-dimensional models. LEED observations of quasicrystalline order have been reported for $Al_{65}Cu_{15}Co_{20}$ surfaces respectively parallel and perpendicular to the periodic axis (McRae *et al.* 1990*b*). With reference to the rotational symmetry of the LEED patterns, these are called the two-fold and ten-fold surfaces respectively.

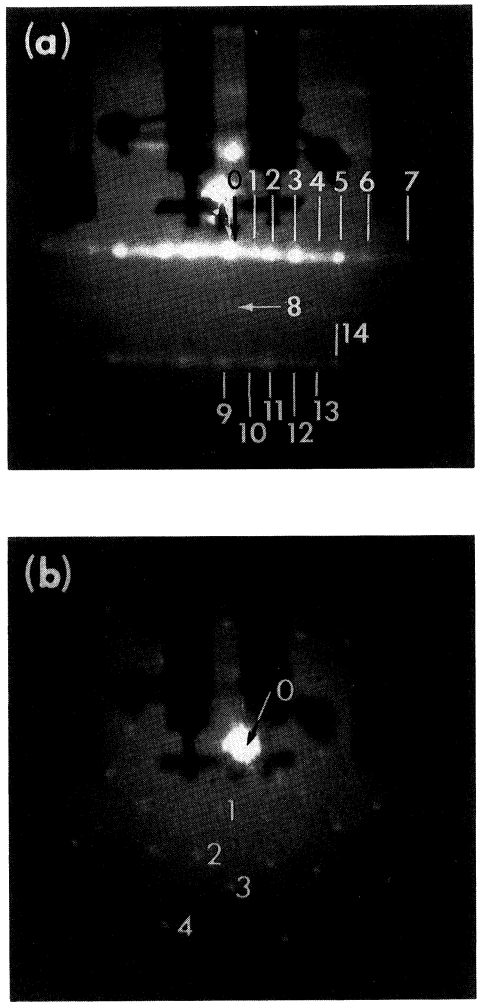

Fig. 13. Conventional LEED patterns from the (a) two-fold and (b) ten-fold surfaces of a decagonal quasicrystal. The numbered spots have been indexed using the structural parameter values given in the text.

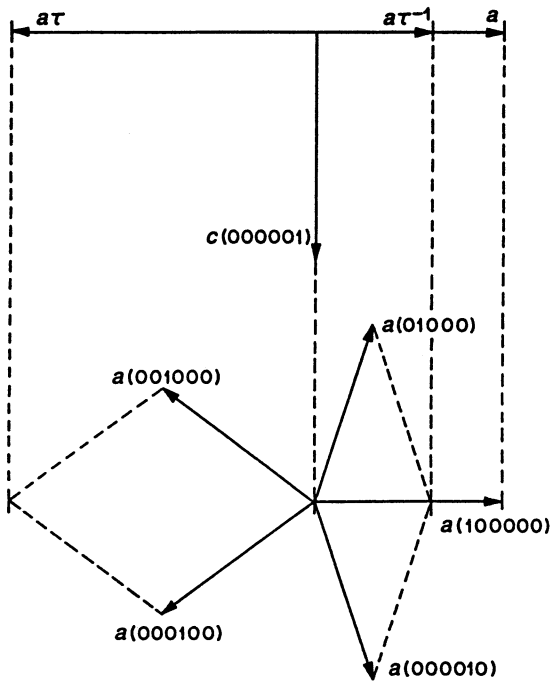

Fig. 14. Basic vectors used to index decagonal quasicrystal diffraction patterns.

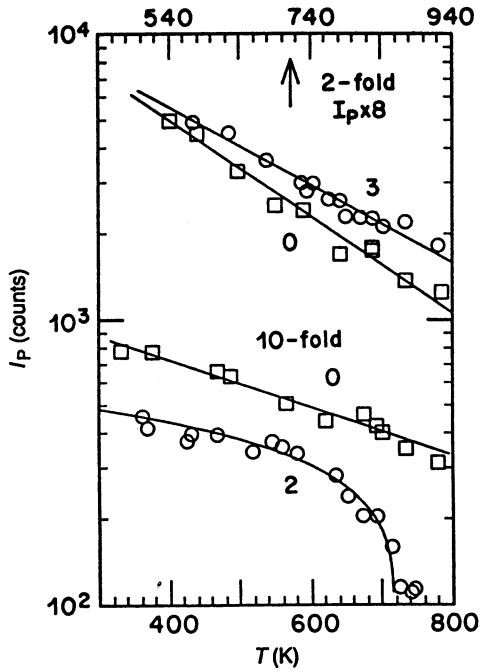

Fig. 15. Dependence of spot peak intensity I_P on sample temperature T in the LEED patterns from the decagonal quasicrystal $Al_{65}Cu_{15}Co_{20}$. The specular spots are identified by 0, nonspecular spots by numerals as in Fig. 13. The curves are fits to data (see text).

Representative room-temperature LEED patterns for the quasicrystal surfaces are shown in Fig. 13. The spots identified by numerals are indexed by a scheme like that used in the presentation of corresponding X-ray diffraction results, and the lengths a and c of the basic vectors (Fig. 14) required to fit the spot positions are the same within error (±5%) as the corresponding values from X-ray diffraction, namely $a = 0 \cdot 63$ Å^{-1} and $c = 2\pi/d$, where $d = 8 \cdot 26$ Å is the spacing of quasicrystalline layers.

Observations of LEED spot peak intensity I_P against sample temperature T (Fig. 15) show that the stability of quasicrystalline ordering at higher T is quite different for the two surfaces studied. When the sample is heated, the intensities of both the specular and non-specular spots in the LEED pattern for the two-fold surface decline like a Debye–Waller factor as illustrated by the straight-line plots in the upper part of Fig. 15. For the ten-fold surface the specular spot intensity also has the Debye–Waller T dependence (plot 10 in the lower part of Fig. 15) but as also illustrated (plot 2) the non-specular spots weaken suddenly with increasing T approaching an apparent critical temperature T_1. The T dependence of the non-specular spot intensities I_P is well represented by an expression of the form

$$I_P(T) - I_P(T_1) \propto (1 - T/T_1)^{2\beta}, \tag{2}$$

where β is a constant critical exponent. A fit to the experimental points (plot 2, Fig. 15) is obtained with parameter values $\beta = 0 \cdot 25 \pm 0 \cdot 02$ and $T_1 = 715 \pm 5$ K. The intensity changes summarised in Fig. 15 were not appreciably delayed on the time-scale of the measurement (100 s at each temperature), nor were they accompanied by any change of either width or shape of the spot profiles. Similarities between these results and those for $Cu_3Au(100)$ (Section 3) and Ge(111) (Section 4) may be noted.

These results have been interpreted as indicating a disordering transition of the ten-fold surface at T_1. The interpretation by a surface and not a bulk transition is required to explain the observation of a transition at the ten-fold but not at the two-fold surface.

With regard to the gross nature of the disordering transition, the observations lead to the following conclusions:

(*a*) The fact that the transition affects only the non-specular spot intensities ($S_{||} \neq 0$) and leaves the specular ones ($S_{||} = 0$) unchanged is an indication that disordering involves atomic displacements primarily parallel to the surface plane [this discussion is similar to that for Ge(111), see Section 4].

(*b*) In view of the high surface sensitivity of LEED, the retention of appreciable non-specular intensity above T_1 suggests that the disordering displacements are limited to one or at most a few of the outermost atom layers.

(*c*) The observation of an intensity variation like that of equation (1) and the absence of pronounced time delay are indications that the transition is second order (see Section 3 for a discussion of the importance of kinetics in the determination of the order of surface phase transitions).

The possible mechanisms of disordering transitions at quasicrystal surfaces include phason disordering (Jaric 1988), as well as the surface melting and roughening mechanisms that have been the subject of recent investigations on ordinary crystals as discussed in Section 4. No detailed theoretical treatment of these mechanisms is available for quasicrystal surfaces. However, the possibility of roughening was considered in a pioneering discussion of the stability of quasicrystal surfaces (Lipowsky and Henley 1988) in which it was argued that the ten-fold surface of an ideal decagonal quasicrystal should disorder at a lower temperature than a two-fold one. The LEED experiment supports the conclusions that the ten-fold surface ordering is relatively unstable, but a roughening mechanism must be ruled out in the present instance because of point (*a*) above. The absence of significant changes of the spot profile is additional evidence against roughening.

Acknowledgments

We thank the organisers of the Interfaces in Molecular, Electron and Surface Physics Workshop for their hospitality and for providing the opportunity to present this paper. We acknowledge financial support to attend the Workshop from the National Science Foundation. We also acknowledge the help of Mr B. K. Murphy in the timely preparation of the manuscript.

References

Allen, S. M., and Cahn, J. W. (1979). *Acta Metall.* **27**, 1085.
Alvarado, S. F., Campagna, M., Fattah, A., and Uelhoff, W. (1987). *Z. Phys.* B **66**, 103.
Binder, K. (1983). 'Phase Transitions and Critical Phenomena', Vol. 8 (Academic: New York).
Buck, T. M., Weatley, G. H., and Marchut, L. (1983). *Phys. Rev. Lett.* **51**, 43.
Cahn, R. W., Siemers, P. A., and Hall, E. L. (1987). *Acta Metall.* **35**, 2753.
Cowley, J. M. (1950). *J. Appl. Phys.* **21**, 24.
Dietrich, S. (1988). 'Phase Transitions and Critical Phenomena', Vol. 12 (Academic: New York).
Dosch, H., Mailander, L., Lied, A., Peisl, J., Grey, F., Johnson, R. L., and Krummacher, S. (1988). *Phys. Rev. Lett.* **60**, 2382.
Fontaine, D. de (1979). 'Solid State Physics', Vol. 34, p. 73 (Academic: New York).
Frantsuzov, A. A., and Makrushin, N. I. (1973). *Surf. Sci.* **40**, 320.
Gompper, G., and Kroll, D. M. (1989). *Phys. Rev.* B **38**, 459.
Hansen, M. (1958). 'Constitution of Binary Alloys' (McGraw–Hill: New York).
Jamison, K. D., Lind, D. M., Dunning, F. B., and Walters, K. G. (1985). *Surf. Sci.* **159**, 451.
Jaric, M. V. (Ed.) (1988). 'Introduction to Quasicrystals' (Academic: New York).
Kortan, A. R., Becker, R. S., Thiel, F. A., and Chen, H. S. (1990). *Phys. Rev. Lett.* **64**, 200.
Kortan, A. R., Thiel, F. A., Chen, H. S., Tsai, A. P., Inoue, A., and Masumoro, T. (1989). *Phys. Rev.* B **40**, 9397.
Kroll, D. M., and Gompper, G. (1987). *Phys. Rev.* B **36**, 7078.
Kropfl, W. J. (1989). Unpublished software development.
Krummacher, S., Sen, N., Gudat, W., Johnson, R., Grey, F., and Ghijsen, J. (1989). *Z. Phys.* B **75**, 235.
Lagally, M. G., and Martin, J. A. (1983). *Rev. Sci. Instrum.* **54**, 1273.
Lagally, M. G., Savage, D. E., and Tringides, M. C. (1988). 'Reflection High-energy Electron Diffraction and Reflection Electron Imaging of Surfaces', p. 139. (Plenum: New York).
Lever, R. F. (1968). *Surf. Sci.* **9**, 370.
Lever, R. F., and Went, H. R. (1970). *Surf. Sci.* **19**, 435.
Lipowsky, R. (1982). *Phys. Rev. Lett.* **49**, 1575.
Lipowsky, R. (1984). *J. Appl. Phys.* **55**, 2485.
Lipowsky, R. (1986). *Ferroelectrics* **73**, 69.
Lipowsky, R., and Gompper, G. (1984). *Phys. Rev.* B **29**, 5213.

Lipowsky, R., and Henley, C. L. (1988). *Phys. Rev. Lett.* **60**, 2394.
Lipowsky, R., Kroll, D. M., and Zia, R. K. P. (1983). *Phys. Rev.* B **27**, 4499.
Ludwig, K. F., Stephenson, G. B., Jordan-Sweet, J. L., Mainville, J., Yang, Y. S., and Sutton, M. (1988). *Phys. Rev. Lett.* **61**, 1859.
McRae, E. G., and Buck, T. M. (1990). *Surf. Sci.* **227**, 67.
McRae, E. G., Buck, T. M., Malic, R. A., Wallace, W. E., and Sanchez, J. M. (1990*a*). *Surf. Sci.* (in press).
McRae, E. G., Landwehr, J. M., McRae, J. E., Gilmore, G. H., and Grabow, M. H. (1988). *Phys. Rev.* B **38**, 13178.
McRae, E. G., and Malic, R. A. (1984). *Surf. Sci.* **148**, 551.
McRae, E. G., and Malic, R. A. (1988). *Phys. Rev.* B **38**, 13163.
McRae, E. G., and Malic, R. A. (1990). *Phys. Rev.* B **42**, 1509.
McRae, E. G., Malic, R. A., and Kapilow, D. A. (1985). *Rev. Sci. Instrum.* **56**, 2077.
McRae, E. G., Malic, R. A., Lalonde, T. H., Thiel, F. A., Chen, H. S., and Kortan, A. R. (1990*b*). Unpublished.
Majia-Lira, F., Bennemann, K. H., and Moran-Lopez, J. L. (1985). *Phys. Rev.* B **32**, 5926.
Malic, R. A. (1988). *Rev. Sci. Instrum.* **59**, 1951.
Moran-Lopez, J. L., Majia-Lira, F., and Bennemann, K. H. (1985). *Phys. Rev. Lett.* **54**, 1936.
Nagler, S. E., Shannon, R. F., Harkless, C. R., Singh, M. A., and Nicklow, R. M. (1988). *Phys. Rev. Lett.* **61**, 718.
Potter, H. C., and Blakely, J. M. (1975). *J. Vac. Sci. Technol.* **12**, 635.
Rase, C. L., and Mikkola, D. E. (1975). *Metall. Trans.* A **6**, 2267.
Sakai, M., and Mikkola, D. E. (1971). *Metall. Trans.* **2**, 1635.
Sanchez, J. M., and Moran-Lopez, J. L. (1985*a*). *Phys. Rev.* B **32**, 3534.
Sanchez, J. M., and Moran-Lopez, J. L. (1985*b*). *Surf. Sci.* **157**, L297.
Sato, H., and Toth, R. S. (1962). *Phys. Rev.* **127**, 469.
Scheithauer, U., Meyer, G., and Henzler, M. (1986). *Surf. Sci.* **178**, 441.
Steinhardt, P. J., and Ostlund, S. (Eds) (1987). 'The Physics of Quasicrystals' (World Scientific: Singapore).
Sundaram, V., S., Alben, R. S., and Robertson, W. D. (1974). *Surf. Sci.* **46**, 653.
Sundaram, V. S., Farrell, B., Alben, R. S., and Robertson, W. D. (1975). *Phys. Rev. Lett.* **31**, 1139.
Van Hove, M. A., Weinberg, W. H., and Chan, C.-M. (1986). 'Low-Energy Electron Diffraction' (Springer: Berlin).
Warren, B. E. (1969). 'X-ray Diffraction', Ch. 13 (Addison–Wesley: Reading, Mass.).
Wilson, A. J. C. (1943). *Proc. R. Soc. London* A **181**, 360.
Yamaguchi, S., Watanabe, D., and Ogawa, S. (1961). *J. Phys. Soc. Jpn* **17**, 1030.

Manuscript received 6 February, accepted 18 June 1990